Influence of Small-Scale Magnetic Field on the Reverse Positron Current in the Inner Gaps of Radio Pulsars

D. P. Barsukov[1,2], O. A. Goglichidze[1], and A. I. Tsygan[1*]

[1]*Ioffe Physical–Technical Institute, Russian Academy of Sciences, St. Petersburg, 194021 Russia*
[2]*Peter the Great St. Petersburg Polytechnic University, St. Petersburg Russia*
Received March 18, 2015; in final form, October 20, 2015

Abstract—The reverse positron current flowing through the inner gap of an old radio pulsar in the presence of a small-scale magnetic field is found. Computations for the case of both strong and weak screening of the longitudinal electric field by the electron–positron plasma are presented.

1. INTRODUCTION

Heating of the polar caps of radio pulsars by the reverse positron current flowing in their inner gaps [1, 2] was first considered in [3]. In models with a vacuum gap, the question arises of the reverse positron current and its influence on heating of the polar caps of radio pulsars; this was considered, e.g., in [4–6]. The formation of the reverse current, as well as its value and its influence on the operation of the inner gap, were investigated in detail in [8] for a model with a free outflow of electrons from the neutron-star surface [7]. It was assumed in [8] that the electron–positron plasma that is created near the upper plate of the gap almost immediately leads to complete screening of the longitudinal electric field [we will call this the strong shielding (SS) model). However, it was shown in [9] that, while it may be difficult to prove that this assertion is incorrect, it is doubtful at the very least. Further, the expressions for the reverse current obtained in [9] differ slightly from those obtained in [8]. It was assumed in [9] that the longitudinal electric field falls off very rapidly in the region occupied by electron–positron plasma, however, this field remains non-zero everywhere (we will call this the weak shielding (WS) model). It was shown in [10] that taking into account variations of the Goldreich–Julian density along the magnetic-field lines [11], $\rho_{GJ} = -\mathbf{\Omega}\tilde{\mathbf{B}}/(2\pi c)$, where $\mathbf{\Omega}$ is the rotational angular velocity of the star, in the WS model [9] leads to a sharp increase in the reverse positron current. In a number of cases, heating of the polar caps becomes so strong that this heating rate exceeds the thermal X-ray luminosity of the neutron star.

The presence and configuration of the small-scale magnetic field is very important for the operation of the inner gap. This field is required for the generation of the electron–positron plasma in some old radio pulsars [12, 13], and arises in a completely natural way in a number of models for the generation of the dipolar magnetic field of the neutron star (see, e.g., [14–17]). The structure of the small-scale magnetic field and its influence on the operation of the inner gap have been considered, for example, in [8, 12, 18–20].

Our current study is a direct continuation of [10, 21]. Our aim was to obtain an expression for the intensity of the heating of the polar caps of old radio pulsars by the reverse positron current for the model [21], which takes into account the influence of small-scale magnetic field, following the method developed in [8].

We treated radio pulsars using the model of Goldreich and Julian [11]. We assumed that particles are accelerated only at the inner gap, which occupies the entire cross section of the pulsar tube, and restricted our consideration to the case when the lower plate of the inner gap is located right at the neutron-star surface (a "polar cap" model) [3, 22]. We assumed that the magnetic field at the neutron-star surface is modest, $B \sim 10^{11} - 10^{13}$ G, and that the strength of the small-scale magnetic field is comparable to the strength of the dipole field. We assumed that the surface is fairly hot at the polar cap, $T \sim (1-3) \times 10^6$ K. It is reasonable to suppose that the inner gap operates in a free-outflow regime for the electrons coming from the neutron-star surface [23], where the electrons flow out more or less uniformly from the entire polar-cap surface, without the generation of sparks. This is more characteristic for a vacuum-gap model [4, 22], which requires small-scale magnetic fields that

*E-mail: tsygan@astro.ioffe.ru

are 10−100 times higher than the dipolar fields [5, 19, 24] or a quark star in place of the neutron star (see, e.g., [25, 26]), or for models for the radiation of radio transients and very old radio pulsars, which are essentially already beyond their switching-off lines (see, e.g., [27, 28]).

We restricted our study to the simplest case when the electron−positron pairs are created via the absorption of curvature radiation (CR) emitted by primary electrons in the presence of a magnetic field (which we will call the CR case). The case when the electron−positron pairs are created mainly via the absorption of non-resonance inverse Compton radiation (NICR) created when thermal photons are scattered on primary electrons in the presence of a magnetic field (the NICR case) was not considered. We also assumed that the inner gap operates in a stationary regime; i.e., all quantities are time independent in a coordinate frame rotating with the neutron star, right out to the light cynder. Moreover, we neglected all general-relativistic effects apart from general-relativistic frame dragging, since this effect makes an appreciable contribution to the electric potential.

2. MAGNETIC FIELD

We used the same model for the non-dipolar magnetic field near the neutron-star surface as in [29] (see also [20, 21, 30, 31]), namely, the magnetic-field near the polar-cap surface was modeled using two dipoles. The first of these dipoles (the main and strongest) $\mathbf{m}$ is located at the center of the neutron star. The angle between the dipole-moment vector $\mathbf{m}$ and the pulsar's rotation axis $\boldsymbol{\Omega}$ is denoted χ. The second dipole $\mathbf{m_1}$ is located near the magnetic pole of the neutron star (its center is located on the axis of the main dipole $\mathbf{m}$), a distance Δa from the surface (inside the star), where a is the radius of the neutron star (see Fig. 1). The vector $\mathbf{m_1}$ is taken to be perpendicular to $\mathbf{m}$. The angle between $\mathbf{m_1}$ and the $(\mathbf{m}, \boldsymbol{\Omega})$ plane is denoted ϕ_Ω. When $\phi_\Omega = 0$, the vector $\mathbf{m_1}$ lies in the $(\mathbf{m}, \boldsymbol{\Omega})$ plane and is directed toward the pulsar's rotation axis (see Fig. 2). We took the parameter Δ to be everywhere equal to 0.1.

We introduce the spherical coordinate system $(\tilde{r}, \tilde{\theta}, \tilde{\phi})$ with its orgin O at the center of the star, where $\tilde{r} = 0$, the Oz axis is directed along $\mathbf{m}$, and the Ox axis is directed along $\mathbf{m_1}$, so that $\mathbf{m} = m\mathbf{e_z}$ and $\mathbf{m_1} = m_1 \mathbf{e_x}$. In this coordinate system, in the approximation of small θ, $\theta \ll 1$, the magnetic field near the neutron-star surface has the form [29]:

$$B_{\tilde{r}} = \frac{B_0}{\eta^3}, \quad B_{\tilde{\theta}} = \frac{B_0}{\eta^3}\left(\frac{\tilde{\theta}}{2} + \mu(\eta)\cos\tilde{\phi}\right), \quad (1)$$
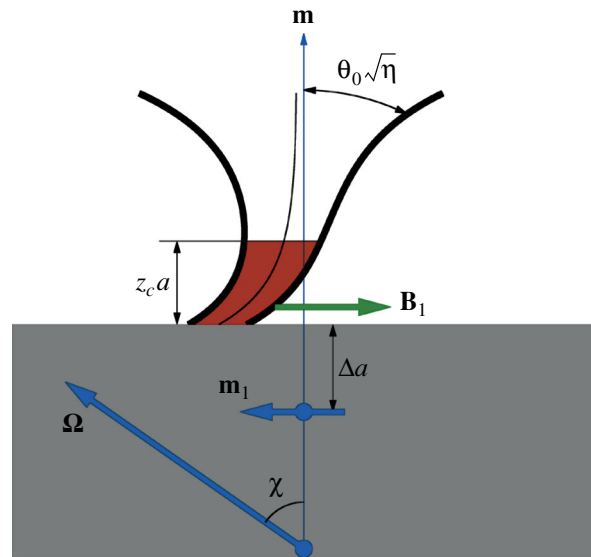

Fig. 1. Arrangement of the inner gap, the main dipole $\mathbf{m}$, and the secondary dipole $\mathbf{m_1}$ in the two-dipole model [29].
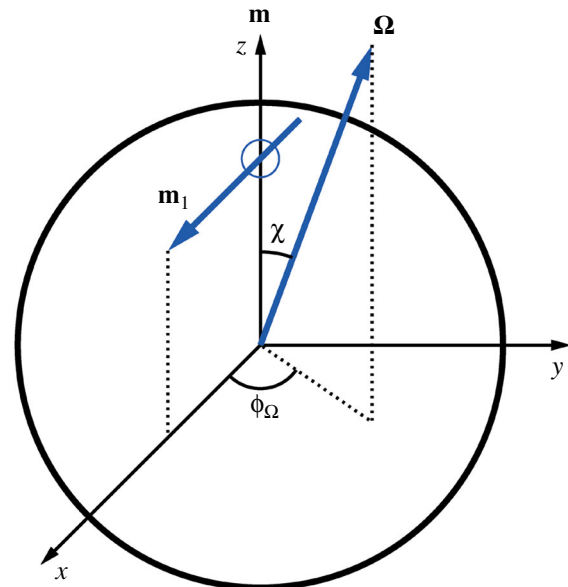

Fig. 2. Orientation of the basis vectors $\mathbf{e_x}, \mathbf{e_y}, \mathbf{e_z}$ in the two-dipole model [29]. The angles χ and ϕ_Ω are indicated.

$$B_{\tilde{\phi}} = -\frac{B_0}{\eta^3}\mu(\eta)\sin\tilde{\phi},$$

where $\mu(\eta) = \nu\left(\frac{\Delta\eta}{\eta - 1 + \Delta}\right)^3$, $\nu = B_1/B_0$, $\eta = \tilde{r}/a$, B_0 and B_1 are the magnetic-field strengths at the magnetic pole of the neutron star ($\eta = 1$, $\tilde{\theta} = 0$, $\tilde{\phi} = 0$) due to the dipoles $\mathbf{m}$ and $\mathbf{m_1}$.

Further, it is convenient to transform from spher-

ical coordinates ($\tilde{r}$, $\tilde{\theta}$, $\tilde{\phi}$) to coordinates tied to the magnetic-field lines (η, ξ, ϕ) [21]. Here, $\eta = \tilde{r}/a$ is the coordinate along the magnetic-field lines. At times, it will be more convenient to use the quantity $z = \eta - 1$. The coordinates ξ and ϕ are labeled according to the magnetic-field lines. When $1 \ll \eta \ll \eta_{LC}$, when the magnetic field can be taken to be essentially dipolar,

$$\sin \tilde{\theta} = \sin \left(\theta_s(\eta) \right) \xi, \quad \tilde{\phi} = \phi. \qquad (2)$$

Further, we assume that, at any height, the cross section of the pulsar tube is a circle with radius $a\theta_s(\eta)$, the line with $\xi = 0$ passes through the center of this circle, and the line with $\xi = 1$ corresponds to the boundary of the pulsar tube. The radius of the pulsar tube $\theta_s(\eta)$ was taken to be given by

$$B(\eta, \xi = 0, \phi = 0)\theta_s^2(\eta) = B_0\theta_0^2, \qquad (3)$$

where $\theta_0 = \sqrt{\Omega a/c}$.

3. CHARGE DENSITY

In place of the number density n, we introduce the dimensionless quantity A:

$$A = \frac{2\pi ce}{\Omega B}n. \qquad (4)$$

The reason for this is that, nearly everywhere in the pulsar tube, the particles move along the magnetic-field lines with speeds close to the speed of light: $\vec{v} \approx \pm c\vec{B}/B$. Then, if a given type of particle doesn't have a source, it follows from the equations

$$\nabla \cdot \vec{j} = 0, \quad \nabla \cdot \vec{B} = 0, \quad \vec{j} = \rho\vec{v}, \qquad (5)$$

that $(\vec{B}, \nabla)A = 0$; i.e., A is constant along the magnetic-field lines, and is therefore independent of z: $A = A(\xi, \phi)$.

We assumed that only primary electrons flowing from the cathode (the neutron-star surface) A_{prim} and positrons in the reverse current A_{rev} are present inside the pulsar diode ($0 < z < z_c$):

$$\rho = \frac{\Omega B}{2\pi c} \left(-A_{\text{prim}} + A_{\text{rev}} \right) \quad \text{with} \quad 0 < z < z_c. \quad (6)$$

Here, we have neglected the presence of tertiary electrons that are created and reversed near the cathode [32].

We also assumed that there is no significant birth or reversal of particles in the region of the pulsar diode, so that A_{prim} and A_{rev} are independent of z when $0 < z < z_c$. This assumption was used, in particular, in [8, 9, 33].

Primary electrons A_{prim}, upward moving secondary electrons $\tilde{A}_-$ and positrons $\tilde{A}_+$, and downward moving positrons of the reverse current $\tilde{A}_{\text{rev}}$ are present above the upper plate of the pulsar diode, $z > z_c$:

$$\rho = \frac{\Omega B}{2\pi c} \left(-A_{\text{prim}} - \tilde{A}_-(z) \right. \qquad (7)$$
$$\left. + \tilde{A}_+(z) + \tilde{A}_{\text{rev}}(z) \right).$$

By definition, the number of primary electrons in this region is constant, $A_{\text{prim}} = \text{const}(z)$. Neglecting the difference of the speed of the secondary particles from the speed of light, we can express the conservation of charge in the form

$$\frac{\partial \tilde{A}_+}{\partial z} = \frac{\partial \tilde{A}_-}{\partial z} - \frac{\partial \tilde{A}_{\text{rev}}}{\partial z}, \qquad (8)$$

which, using the condition $\tilde{A}_-|_{z=z_c} = 0$, $\tilde{A}_+|_{z=z_c} = 0$, $\tilde{A}_{\text{rev}}|_{z=z_c} = A_{\text{rev}}$, enables us to write $\tilde{A}_-(z) - \tilde{A}_+(z) = A_{\text{rev}} - \tilde{A}_{\text{rev}}(z)$, so that

$$\rho = \frac{\Omega B}{2\pi c} \left(-A_{\text{prim}} - A_{\text{rev}} + 2\tilde{A}_{\text{rev}}(z) \right). \qquad (9)$$

4. MODEL OF A THIN TUBE

Let us suppose that $\theta_s \ll \Delta$. The Poisson equation (in a coordinate frame rotating with the neutron star) [79, 34, 35],

$$\Delta \Phi = -4\pi(\rho - \rho_{GJ}), \qquad (10)$$

can then be written in the form [35]

$$\frac{\partial^2 \Phi}{\partial z^2} + \frac{1}{\theta_s^2(\eta)}\Delta_\perp\Phi \qquad (11)$$
$$= -4\pi\frac{\Omega B(\eta)}{2\pi c}a^2(A + f(\eta)),$$

where A is the dimensionless total charge density, $f(\eta) = -\frac{2\pi c}{\Omega B(\eta)}\rho_{GJ}$ is (within its sign) the dimensionless Goldreich−Julian density, and

$$\Delta_\perp\Phi = \frac{1}{\xi}\frac{\partial}{\partial \xi}\left(\xi\frac{\partial \Phi}{\partial \xi}\right) + \frac{1}{\xi^2}\frac{\partial^2 \Phi}{\partial \phi^2}. \qquad (12)$$

We obtain using (3)

$$\theta_s^2(\eta)\frac{\partial^2 \Phi}{\partial z^2} + \Delta_\perp\Phi = 2\Phi_0(A + f(\eta)), \qquad (13)$$

where $\Phi_0 = \frac{\Omega Flux}{\pi c} = \text{const}(z)$.

We specified the boundary conditions as follows [8]:

$$\Phi|_{z=0} = 0, \quad \Phi|_{\xi=1} = 0, \qquad (14)$$
$$\Phi|_{\xi=0} \text{—finite},$$

$$\left.\frac{\partial \Phi}{\partial z}\right|_{z=0} = 0, \qquad (15)$$

$$\left.\frac{\partial \Phi}{\partial z}\right|_{z=z_c} = \epsilon(\xi, \phi). \qquad (16)$$

The conditions (14) express the continuity of the potential Φ. The condition (15) corresponds to a regime with free outflow from the neutron-star surface, and the condition (16) specifies the value of the longitudinal electric field at the upper plate.

In most cases, the specification of a particular value of $\epsilon(\xi, \phi)$ is determined by the definition of the height of the upper plate z_c. The height z_c is usually chosen so that $\epsilon(\xi, \phi) = 0$. However, in our case, this choice is not very convenient, since the reversal of the electron—positron pairs near the point $z = z_c$ strongly distorts the electric field $\frac{\partial \Phi}{\partial z}$ and, especially, $\frac{\partial^2 \Phi}{\partial z^2}$. As a result, these quantities cannot be determined using the solution inside the gap. Therefore, we preferred to define the height of the upper plate as the greatest height at which the birth and reversal of positrons does not yet appreciably influence the potential Φ. Essentially, we are using the definition of the height of the upper plate of the gap z_c as the height of the "pair formation front", given in [9, 32].

As was shown in [8—10], in the CR case, both heights nearly coincide, and $\epsilon(\xi, \phi)$ can be taken to be much less than the characteristic longitudinal electric field $\frac{\partial \Phi}{\partial z}$ inside the pulsar diode, which, generally speaking, makes it possible to take this quantity to be equal to zero. Note, however, that, in the NICR case, the quantity $\epsilon(\xi, \phi)$ we have introduced will be comparable to the field inside the pulsar diode [33].

Further, when considering the potential inside the gap, we assumed that $f(\eta)$ and ϵ are independent of the azimuthal angle ϕ. Accordingly, the potential Φ is also independent of ϕ. We present the function $\epsilon(\xi)$ in the form of the series

$$\epsilon(\xi) = \sum_{i=1}^{\infty} \epsilon_i \frac{2}{k_i J_1(k_i)} J_0(k_i \xi), \qquad (17)$$

where k_i are the roots of the equation $J_0(k) = 0$.

We used the expression for the magnetic field (1) when computing the function $f(\eta)$. Moreover, we neglected the ξ- and ϕ-dependent "Arons term" $\theta_s(\eta) \xi \cos \phi \sin \chi$, and took $f(\eta)$ to be [21, 36]

$$f(\eta) = \frac{1}{\sqrt{1 + \mu^2(\eta)}} \left(\left(1 - \frac{\kappa}{\eta^3}\right) \cos \chi \qquad (18) \right.$$
$$\left. - \mu(\eta) \left(1 + \frac{1}{2}\frac{\kappa}{\eta^3}\right) \sin \chi \cos \phi_\Omega \right),$$

where the coefficient $\kappa \approx 0.15$ describes the effect of the frame dragging.

4.1. Small Heights

Let us consider the special case $z_c \ll \Delta$. The quantities $f(\eta)$ and $\theta_s(\eta)$ then vary only weakly inside the pulsar diode, and we can write

$$f(\eta) \approx f(1) + \frac{\partial f}{\partial \eta}(1) z, \quad \theta_s(\eta) \approx \theta_s(1). \qquad (19)$$

Equation (13) then acquires the form

$$\theta_s^2(1) \frac{\partial^2 \Phi}{\partial z^2} + \frac{1}{\xi}\frac{\partial}{\partial \xi}\left(\xi \frac{\partial \Phi}{\partial \xi}\right) \qquad (20)$$
$$= -2\Phi_0 \left(A + f(1) + \frac{\partial f}{\partial \eta}(1) z\right).$$

The solution of this equation with the boundary conditions (14)—(16) has the form

$$\Phi = \frac{1}{2}\Phi_0 \frac{\partial f}{\partial \eta}(1) \bigg(z\left(1 - \xi^2\right) \qquad (21)$$
$$- 8\theta_s(1) \sum_{i=1}^{\infty} F_i \frac{J_0(k_i \xi)}{k_i^4 J_1(k_i)} \bigg),$$

$$A = -f(1) - 2\frac{\partial f}{\partial \eta}(1)\theta_s(1) \qquad (22)$$
$$\times \sum_{i=1}^{\infty} \left(\text{th}\left(\frac{\tilde{\gamma}_i z_c}{2}\right) + \frac{\tilde{\epsilon}_i}{\text{sh}(\tilde{\gamma}_i z_c)}\right) \frac{J_0(k_i \xi)}{k_i^2 J_1(k_i)},$$

where

$$F_i = \frac{\left(1 - e^{-\tilde{\gamma}_i z}\right)}{\left(1 + e^{-\tilde{\gamma}_i z_c}\right)} \qquad (23)$$
$$\times \left(1 + e^{-\tilde{\gamma}_i(z_c - z)} \left(1 - \tilde{\epsilon}_i \frac{\left(1 - e^{-\tilde{\gamma}_i z}\right)}{\left(1 - e^{-\tilde{\gamma}_i z_c}\right)}\right)\right),$$

$$\tilde{\epsilon}_i = \frac{\epsilon_i k_i^2}{2\Phi_0 \frac{\partial f}{\partial \eta}(1)}, \quad \tilde{\gamma}_i = \frac{k_i}{\theta_s(1)}. \qquad (24)$$

Hence, we obtain

$$\Phi|_{z=z_c} = \frac{1}{2}\Phi_0 \frac{\partial f}{\partial \eta}(1) \bigg(z_c\left(1 - \xi^2\right) \qquad (25)$$
$$- 8\theta_s(1) \sum_{i=1}^{\infty} \text{th}\left(\frac{\tilde{\gamma}_i z_c}{2}\right)(2 - \tilde{\epsilon}_i) \frac{J_0(k_i \xi)}{k_i^4 J_1(k_i)} \bigg),$$

$$\theta_s^2(1)\left.\frac{\partial^2 \Phi}{\partial z^2}\right|_{z=z_c} = -4\Phi_0 \frac{\partial f}{\partial \eta}(1)\theta_s(1) \qquad (26)$$
$$\times \sum_{i=1}^{\infty} \left(\text{th}\left(\frac{\tilde{\gamma}_i z_c}{2}\right) - \tilde{\epsilon}_i \text{cth}(\tilde{\gamma}_i z_c)\right) \frac{J_0(k_i \xi)}{k_i^2 J_1(k_i)}.$$

Note that, in the special case $\epsilon = 0$, the following condition is automatically satisfied:

$$\theta_s^2(1)\left.\frac{\partial^2 \Phi}{\partial z^2}\right|_{z=z_c} = 2\Phi_0(A + f(1)). \qquad (27)$$

4.2. Large Heights

Now let us consider the case $z_c \gg \theta_s$. Then, apart from regions near the upper and lower plates, the potential Φ is approximately [9, 21]

$$\Phi = \frac{1}{2}\Phi_0 \left(A + f(\eta)\right)\left(1 - \xi^2\right). \qquad (28)$$

When $A \approx -f(1)$, this expression satisfies the boundary conditions for the potential (14), but not those for its derivative (15), (16). Therefore, we add two terms that do not significantly change the potential, but strongly influence the derivatives near the gap plates:

$$\Phi = \frac{1}{2}\Phi_0 \left(A + f(\eta)\right)\left(1 - \xi^2\right) \qquad (29)$$

$$+ \sum_{i=1}^{\infty} \frac{2\Phi_0}{k_i^2} \left(C_i e^{-\gamma_i(z_c - z)} + D_i e^{-\tilde{\gamma}_i z}\right)$$

$$\times \frac{2}{k_i J_1(k_i)} J_0(k_i \xi),$$

where $\gamma_i = k_i/\theta_s(\eta_c)$ and $\tilde{\gamma}_i = k_i/\theta_s(1)$.

Since we assume here $z_c/\theta_s \gg 1$, it makes sense to include the terms with C_i only near the upper plate, $z \approx z_c$, and to include the terms with D_i only near the lower plate, $z \approx 0$. Then, taking into account the boundary conditions (14)–(16), we obtain

$$\Phi = \frac{1}{2}\Phi_0 \left(f(\eta) - f(1)\right)\left(1 - \xi^2\right) \qquad (30)$$

$$- 4\Phi_0 \left(\frac{\partial f}{\partial \eta}(1)\theta_s(1) \sum_{i=1}^{\infty} \left(1 - e^{-\tilde{\gamma}_i z}\right) \frac{J_0(k_i \xi)}{k_i^4 J_1(k_i)}\right)$$

$$- 4\Phi_0 \left(\frac{\partial f}{\partial \eta}(\eta_c)\theta_s(\eta_c) \sum_{i=1}^{\infty} e^{-\gamma_i(z_c - z)}\right.$$

$$\left. \times (1 - \hat{\epsilon}_i) \frac{J_0(k_i \xi)}{k_i^4 J_1(k_i)}\right),$$

$$A = -f(1) - 2\frac{\partial f}{\partial \eta}(1)\theta_s(1) \sum_{i=1}^{\infty} \frac{J_0(k_i \xi)}{k_i^2 J_1(k_i)}, \qquad (31)$$

where $\hat{\epsilon}_i = (\epsilon_i k_i^2)/(2\Phi_0 \frac{\partial f}{\partial \eta}(\eta_c))$. This immediately yields

$$\Phi|_{z=z_c} = \frac{1}{2}\Phi_0 \left(f(\eta_c) - f(1)\right)\left(1 - \xi^2\right) \qquad (32)$$

$$- 4\Phi_0 \left(\frac{\partial f}{\partial \eta}(1)\theta_s(1) \sum_{i=1}^{\infty} \frac{J_0(k_i \xi)}{k_i^4 J_1(k_i)}\right.$$

$$\left. + \frac{\partial f}{\partial \eta}(\eta_c)\theta_s(\eta_c) \sum_{i=1}^{\infty} (1 - \hat{\epsilon}_i) \frac{J_0(k_i \xi)}{k_i^4 J_1(k_i)}\right),$$

$$\theta_s^2(\eta_c) \left.\frac{\partial^2 \Phi}{\partial z^2}\right|_{z=z_c} = \Phi_0 \left(\frac{1}{2}\theta_s^2(\eta_c)\frac{\partial^2 f}{\partial \eta^2}(\eta_c)\right. \qquad (33)$$

$$\left. - 4\frac{\partial f}{\partial \eta}(\eta_c)\theta_s(\eta_c) \sum_{i=1}^{\infty} (1 - \hat{\epsilon}_i) \frac{J_0(k_i \xi)}{k_i^2 J_1(k_i)}\right).$$

If we can neglect terms with $\hat{\epsilon}_i$ and $\frac{\partial f}{\partial \eta}(\eta_c) \gg \theta_s(\eta_c)\frac{\partial^2 f}{\partial \eta^2}(\eta_c)$, these expressions can be written in the form

$$\Phi|_{z=z_c} = \frac{1}{2}\Phi_0 \left(f(\eta_c) - f(1)\right)\left(1 - \xi^2\right) \qquad (34)$$

$$- 4\Phi_0 \left(\frac{\partial f}{\partial \eta}(1)\theta_s(1) + \frac{\partial f}{\partial \eta}(\eta_c)\theta_s(\eta_c)\right) \sum_{i=1}^{\infty} \frac{J_0(k_i \xi)}{k_i^4 J_1(k_i)},$$

$$\theta_s^2(\eta_c) \left.\frac{\partial^2 \Phi}{\partial z^2}\right|_{z=z_c} \qquad (35)$$

$$= -4\Phi_0 \frac{\partial f}{\partial \eta}(\eta_c)\theta_s(\eta_c) \sum_{i=1}^{\infty} \frac{J_0(k_i \xi)}{k_i^2 J_1(k_i)}.$$

When $\theta_s \ll z_c \ll \Delta$, expressions (25) and (26) are transformed into (32) and (33), making it possible to combine them:

$$\Phi|_{z=z_c} = \frac{1}{2}\Phi_0 \left(f(\eta_c) - f(1)\right)\left(1 - \xi^2\right) \qquad (36)$$

$$- 4\Phi_0 \left(\frac{\partial f}{\partial \eta}(1)\theta_s(1) \sum_{i=1}^{\infty} \text{th}\left(\frac{\gamma_i z_c}{2}\right) \frac{J_0(k_i \xi)}{k_i^4 J_1(k_i)}\right)$$

$$- 4\Phi_0 \left(\frac{\partial f}{\partial \eta}(\eta_c)\theta_s(\eta_c) \sum_{i=1}^{\infty} \text{th}\left(\frac{\gamma_i z_c}{2}\right)\right.$$

$$\left. \times (1 - \hat{\epsilon}_i) \frac{J_0(k_i \xi)}{k_i^4 J_1(k_i)}\right),$$

$$\theta_s^2(\eta_c) \left.\frac{\partial^2 \Phi}{\partial z^2}\right|_{z=z_c} = \frac{1}{2}\Phi_0 \theta_s^2(\eta_c)\frac{\partial^2 f}{\partial \eta^2}(\eta_c) \qquad (37)$$

$$- 4\Phi_0 \frac{\partial f}{\partial \eta}(\eta_c)\theta_s(\eta_c)$$

$$\times \sum_{i=1}^{\infty} \left(\text{th}\left(\frac{\gamma_i z_c}{2}\right) - \hat{\epsilon}_i \text{cth}\left(\gamma_i z_c\right)\right) \frac{J_0(k_i \xi)}{k_i^2 J_1(k_i)}.$$

When $\epsilon \equiv 0$ and $\frac{\partial f}{\partial \eta}(\eta_c) \gg \theta_s(\eta_c)\frac{\partial^2 f}{\partial \eta^2}(\eta_c)$, expressions (36) and (37) simplify:

$$\Phi|_{z=z_c} = \frac{1}{2}\Phi_0 \left(f(\eta_c) - f(1)\right)\left(1 - \xi^2\right) \qquad (38)$$

$$- 4\Phi_0 \left(\frac{\partial f}{\partial \eta}(1)\theta_s(1) + \frac{\partial f}{\partial \eta}(\eta_c)\theta_s(\eta_c)\right)$$

$$\times \sum_{i=1}^{\infty} \text{th}\left(\frac{\gamma_i z_c}{2}\right) \frac{J_0(k_i \xi)}{k_i^4 J_1(k_i)},$$

$$\theta_s^2(\eta_c) \left.\frac{\partial^2 \Phi}{\partial z^2}\right|_{z=z_c} = -4\Phi_0 \frac{\partial f}{\partial \eta}(\eta_c)\theta_s(\eta_c) \quad (39)$$

$$\times \sum_{i=1}^{\infty} \text{th}\left(\frac{\gamma_i z_c}{2}\right) \frac{J_0(k_i\xi)}{k_i^2 J_1(k_i)}.$$

5. COMPUTATION OF THE REVERSE CURRENT

We computed the reverse current in precisely the same way as in [8]. As in [8], we took into account the fact that the electron−positron plasma nearly completely screens the longitudinal electric field above the upper plate of the gap, $E_{\parallel} = (\vec{E}, \vec{B})/B$ [8, 9]. Therefore, beginning from some height $z_r^0 > z_c$, we can assume that $\frac{\partial \Phi}{\partial z}$ is small, and the term $\theta_s^2(\eta)\frac{\partial^2 \Phi}{\partial z^2}$ is much smaller than the remaining terms in (13). Accordingly, we assumed that, when $z \geq z_r^0$, Eq. (13) can be written:

$$\Delta_\perp \Phi = -2\Phi_0\left(A + f(\eta)\right). \quad (40)$$

In the CR case, the height z_r^0 is usually very close to the height of the upper plate z_c ($z_r^0 - z_c \ll \theta_s$) [8, 9]. On the contrary, in the NICR case, it is quite possible that $z_r^0 - z_c \sim z_c$ [33].

Let us consider some point $z = z_r \geq z_r^0$ (we will discuss the choice of z_r below) and suppose that only upward moving primary electrons, secondary electrons and positrons, and downward moving positrons in the reverse current are present when $z_c \leq z \leq z_r$. We also assume here that, when $z_r^0 \leq z \leq z_r$, Eq. (40) is satisfied due to the reversal of the secondary positrons (or, if you like, their reversal brings about the screening of the longitudinal electric field $E_{\parallel}$). Using (6) and (9), we can then write the two equations [8, 29]:

$$\theta_s^2(\eta_c) \left.\frac{\partial^2 \Phi}{\partial z^2}\right|_{z=z_c} + \left.\Delta_\perp \Phi\right|_{z=z_c} \quad (41)$$

$$= -2\Phi_0\left(-A_{\text{prim}} + A_{\text{rev}} + f(\eta_c)\right),$$

$$\left.\Delta_\perp \Phi\right|_{z=z_r} = -2\Phi_0\Big(-A_{\text{prim}} \quad (42)$$

$$- A_{\text{rev}} + 2\tilde{A}_{\text{rev}}(z_r) + f(\eta_r)\Big).$$

Subtracting one from the other yields

$$A_{\text{rev}} = \tilde{A}_{\text{rev}}(z_r) + \frac{1}{2}\left(f(\eta_r) - f(\eta_c)\right) \quad (43)$$

$$- \frac{1}{4\Phi_0}\theta_s^2(\eta_c) \left.\frac{\partial^2 \Phi}{\partial z^2}\right|_{z=z_c}$$

$$- \frac{1}{4\Phi_0}\left(\left.\Delta_\perp \Phi\right|_{z=z_c} - \left.\Delta_\perp \Phi\right|_{z=z_r}\right).$$

As is shown in [8, 9] (see also [10]), in the CR case, we can assume that

$$\theta_s^2(\eta_c) \left.\frac{\partial^2 \Phi}{\partial z^2}\right|_{z=z_c} \gg \left.\Delta_\perp \Phi\right|_{z=z_c} - \left.\Delta_\perp \Phi\right|_{z=z_r}. \quad (44)$$

Note that the condition (44) essentially means that the potential drop between $z = z_r$ and $z = z_c$ is much less than the potential drop in the region $z_c - \theta_s < z < z_c$. Therefore, taking (44) to be valid [8], we can write

$$A_{\text{rev}} = \tilde{A}_{\text{rev}}(z_r) + \frac{1}{2}\left(f(\eta_r) - f(\eta_c)\right) \quad (45)$$

$$- \frac{1}{4\Phi_0}\theta_s^2(\eta_c) \left.\frac{\partial^2 \Phi}{\partial z^2}\right|_{z=z_c},$$

where $\theta_s^2(\eta_c) \left.\frac{\partial^2 \Phi}{\partial z^2}\right|_{z=z_c}$ is computed using (39).

5.1. Model with Strong Screening

It was shown in [8] that there is a point at $z > z_c$, $z = z_r^{SS}$, where

$$\left.\frac{\partial \Phi}{\partial z}\right|_{z=z_r^{SS}} = 0, \qquad \left.\frac{\partial^2 \Phi}{\partial z^2}\right|_{z=z_r^{SS}} = 0. \quad (46)$$

It was assumed in [8] that the longitudinal field is screened by the reversal of the positrons in the region $z_c < z < z_r^{SS}$. Above the point z_r^{SS}, there is no reversal of the positrons [8],

$$\tilde{A}_{\text{rev}}(z_r^{SS}) = 0. \quad (47)$$

It was shown in [8] that $z_r^{SS} - z_c \ll \theta_s$ (the CR case was considered in [8]). This means that the term $\frac{1}{2}\left(f(\eta_r^{SS}) - f(\eta_c)\right)$ can be neglected in (45). Consequently, the reverse positron current becomes

$$A_{\text{rev}}^{SS} = -\frac{1}{4\Phi_0}\theta_s^2(\eta_c) \left.\frac{\partial^2 \Phi}{\partial z^2}\right|_{z=z_c}. \quad (48)$$

Substituting (39) into this expression, we find that the reverse positron current is very small, $A_{\text{rev}}^{SS} \sim \frac{\partial f}{\partial \eta}(\eta_c)\theta_s(\eta_c) \sim 10^{-4}$–$10^{-2}$:

$$A_{\text{rev}}^{SS} = \frac{\partial f}{\partial \eta}(\eta_c)\theta_s(\eta_c) \sum_{i=1}^{\infty} \text{th}\left(\frac{\gamma_i z_c}{2}\right) \frac{J_0(k_i\xi)}{k_i^2 J_1(k_i)}. \quad (49)$$

In the limiting cases $z_c \gg \theta_s(\eta_c)$ and $z_c \ll \theta_s(\eta_c)$, Eq. (49) takes the form [9]:

$$A_{\text{rev}}^{SS} \approx \frac{4}{15}\frac{\partial f}{\partial \eta}(\eta_c)\theta_s(\eta_c)\left(1 - \xi^{2.19}\right)^{0.705} \quad (50)$$

$$\text{when} \quad z_c \gg \theta_s(\eta_c),$$

$$A_{\text{rev}}^{SS} \approx \frac{1}{4}\frac{\partial f}{\partial \eta}(1)z_c \quad \text{when} \quad z_c \ll \theta_s(\eta_c). \quad (51)$$

In the case of a purely dipolar magnetic field $\nu = 0$, these expressions acquire the form [9, 12, 29]

$$A_{\text{rev}}^{SS} \approx \frac{4}{5} \frac{\kappa}{\eta_c^{7/2}} \theta_0 \cos\chi \left(1 - \xi^{2.19}\right)^{0.705} \quad (52)$$

$$\text{when } z_c \gg \theta_s(\eta_c),$$

$$A_{\text{rev}}^{SS} \approx \frac{3}{4} \kappa z_c \cos\chi \quad \text{when } z_c \ll \theta_s(\eta_c). \quad (53)$$

Note also that, when $\xi = 0$, A_{rev}^{SS} can be approximated by the following expression, with accuracy to within 5%:

$$A_{\text{rev}}^{SS} \approx \frac{\partial f}{\partial \eta}(\eta_c)\theta_s(\eta_c)F\left(\frac{z_c}{\theta_s(\eta_c)}\right), \quad (54)$$

where $F(x) = \frac{4x}{16+15x}\left(1 + 1.19\frac{x}{1+x^2}\right)$, and $F(x) \approx \frac{x}{4}$ when $x \ll 1$ and $F(x) \approx \frac{4}{15}$ when $x \gg 1$.

5.2. Model with Weak Screening

It was shown in [9] that the conditions (46) cannot all be satisfied simultaneously at the same point. In this connection, it was proposed in [9] to use a single condition in place of the two conditions (46):

$$\Phi \to \Phi_\infty \quad \text{when } \eta \to +\infty. \quad (55)$$

It was also assumed that there were no additional sources of charge anywhere and that the longitudinal electric field was everywhere screened due to the reversal of the positrons. Consequently, generally speaking, all heights from the upper plate to the light cylinder contribute to the reverse current [37, 38].

We interpret the condition (55) as follows. Above the upper plate of the gap at heights $\eta_r^0 < \eta \le \eta_r^{WS}$, the longitudinal electric field is small, and the screening condition (40) is satisfied with good accuracy. This screening is due to the reversal of the positrons. Let us suppose that $\tilde{A}_{\text{rev}}(\eta_r^{WS}) = 0$; i.e., there is no reversal of the positrons at $\eta > \eta_r^{WS}$, and no reverse positron current due to the light cylinder [1, 39]. Setting $\eta_r = \eta_r^{WS}$ in (45), we then obtain

$$A_{\text{rev}}^{WS} = \frac{1}{2}\left(f(\eta_r^{WS}) - f(\eta_c)\right) \quad (56)$$

$$- \frac{1}{4\Phi_0}\theta_s^2(\eta_c)\left.\frac{\partial^2 \Phi}{\partial z^2}\right|_{z=z_c}.$$

We will now say a few words about the choice of the height η_r^{WS}. First of all, it is reasonable to choose η_r^{WS} to be somewhat lower than the height $\eta_{\text{rad}} \sim 10^1 - 10^2$, where the plasma oscillations are intense enough to influence the motions of particles [40−43]. In the case of field lines that are unfavorable according to the criterion of Arons, the height η_r^{WS}

should not exceed the height η_{max}, where the function $f(\eta)$ reaches its maximum value, and above which it is necessary to constantly add an additional positive charge, rather than adding a negative charge (due to the reversal of the positrons). In the case of a purely dipolar magnetic field ($\nu = 0$), we have

$$\eta_{\text{max}} \approx \left(-\frac{6\kappa}{\theta_0\xi}\frac{\cot\chi}{\cos\phi}\right)^{2/7} \sim 2-3. \quad (57)$$

Based on the above arguments, it seems reasonable to us to take $\eta_r^{WS} \sim \min(\eta_{\text{max}}, \eta_{\text{rad}}) \sim 3-50$. At such heights, we can assume that the magnetic field differs only weakly from a dipolar field, and that we can neglect the "Arons term" $\theta_s(\eta)\xi\cos\phi\sin\chi$ when computing $f(\eta)$. Consequently, we can set in (56)

$$f(\eta_r^{WS}) \approx (1-\kappa)\cos\chi. \quad (58)$$

We thus immediately obtain

$$A_{\text{rev}}^{WS} = \frac{1}{2}\left((1-\kappa)\cos\chi - f(\eta_c)\right) + A_{\text{rev}}^{SS}. \quad (59)$$

Since the first term is usually much greater than the second, we can write

$$A_{\text{rev}}^{WS} \approx \frac{1}{2}\left((1-\kappa)\cos\chi - f(\eta_c)\right). \quad (60)$$

6. HEATING OF THE POLAR CAP

We estimated the heating of the polar cap of the pulsar using the formula

$$L_{\text{tot}} = \int_0^1 \frac{c}{e} \rho_{\text{rev}}|_{z=0}\, e\, \left.\Phi\right|_{z=z_c} \theta_s^2(1)a^2 2\pi\xi d\xi. \quad (61)$$

Substituting $\rho_{\text{rev}}|_{z=0} = \frac{\Omega B(1)}{2\pi c}A_{\text{rev}}$ and taking into account that $Flux = \pi\theta_s^2(1)a^2 B(1)$ and $\Phi_0 = \frac{\Omega Flux}{\pi c}$, we find

$$L_{\text{tot}} = c\Phi_0^2 \int_0^1 A_{\text{rev}} \left.\frac{\Phi}{\Phi_0}\right|_{z=z_c} \xi d\xi. \quad (62)$$

We obtain in the SS model using (49) and (38)

$$L_{\text{tot}}^{SS} = c\Phi_0^2 2\frac{\partial f}{\partial \eta}(\eta_c)\theta_s(\eta_c) \quad (63)$$

$$\times \left((f(\eta_c) - f(1)) F_0\left(\frac{z_c}{\theta_s(\eta_c)}\right) \right.$$

$$- \left(\frac{\partial f}{\partial \eta}(1)\theta_s(1) + \frac{\partial f}{\partial \eta}(\eta_c)\theta_s(\eta_c)\right)$$

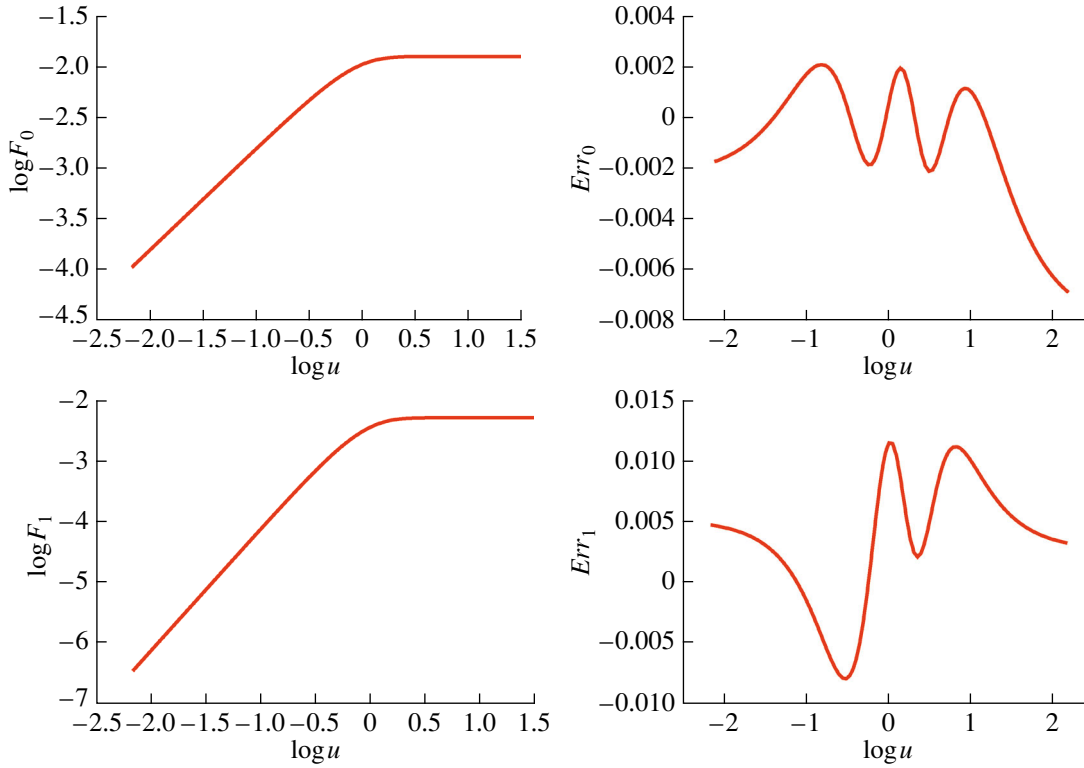$$\left. \times F_1\left(\frac{z_c}{\theta_s(\eta_c)}\right)\right).$$

Fig. 3. Left: plots of the functions $F_0(u)$ (upper) and $F_1(u)$ (lower) computed using (65) and (66). Right: the corresponding relative errors $Err_A = (F_A - F_A^{app})/F_A$, $A = 0, 1$. The approximations were obtained using (67) and (68), respectively.

We obtain in the WS model using (59) and (38)

$$L_{\text{tot}}^{WS} = L_{\text{tot}}^{SS} + \frac{1}{16}c\Phi_0^2\left(f(\eta_r^{WS}) - f(\eta_c)\right) \quad (64)$$

$$\times \left((f(\eta_c) - f(1)) - 32\left(\frac{\partial f}{\partial \eta}(1)\theta_s(1)\right.\right.$$

$$\left.\left. + \frac{\partial f}{\partial \eta}(\eta_c)\theta_s(\eta_c)\right)F_0\left(\frac{z_c}{\theta_s(\eta_c)}\right)\right),$$

where the functions $F_0(u)$ and $F_1(u)$ are given by

$$F_0(u) = \sum_{i=1}^{\infty} \frac{1}{k_i^5}\text{th}\left(\frac{k_i u}{2}\right), \quad (65)$$

$$F_1(u) = \sum_{i=1}^{\infty} \frac{1}{k_i^6}\text{th}^2\left(\frac{k_i u}{2}\right). \quad (66)$$

Plots of the functions $F_0(u)$ and $F_1(u)$ are shown in Fig. 3. When $u \ll 1$, it is obvious that $F_0(u) \approx K_f\frac{u}{2}$ and $F_1(u) \approx K_f\left(\frac{u}{2}\right)^2$, where $K_f = \sum_{i=1}^{\infty}\frac{1}{k_i^4} = \frac{1}{32}$. Accordingly, when $u \gg 1$, $F_0(u) \approx \sum_{i=1}^{\infty}\frac{1}{k_i^5} \approx 1.27 \times 10^{-2}$ and $F_1(u) \approx \sum_{i=1}^{\infty}\frac{1}{k_i^6} = \frac{1}{192}$. In the interval

$10^{-2} \leq u \leq 10^2$, these functions can be approximated by the following expressions with accuracy to within 1.5%:

$$F_0(u) \approx F_0^{app}(u) \quad (67)$$

$$= a_0 u\frac{1 + b_0 u + c_0 u^2}{1 + d_0 u + e_0 u^2 + h_0 u^3},$$

$$F_1(u) \approx F_1^{app}(u) = \frac{a_1 u}{1 + b_1 u}\frac{1 + c_1 u + d_1 u^2}{1 + e_1 u + h_1 u^2}. \quad (68)$$

The values of the coefficients in these expressions are given in the table. The right-hand panels of Fig. 3 show the relative errors obtained with this approx-

Values of the coefficients in (67) and (68)

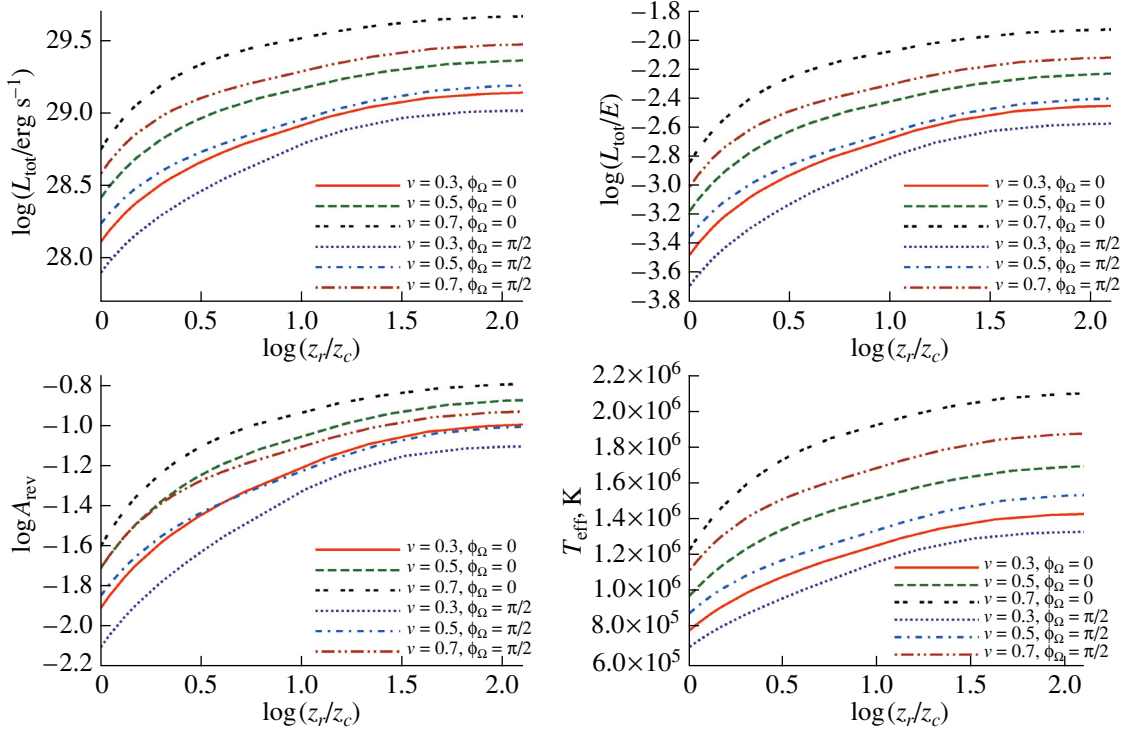| Coeff-icient	Value	Coeff-icient	Value
a_0	1.566×10^{-2}	a_1	7.772×10^{-3}
b_0	5.556×10^{-1}	b_1	1.195
c_0	4.692×10^{-1}	c_1	-3.496×10^{-1}
d_0	6.271×10^{-1}	d_1	2.067×10^{-1}
e_0	7.920×10^{-1}	e_1	-4.147×10^{-1}
h_0	5.759×10^{-1}	h_1	2.588×10^{-1}

Fig. 4. Upper: dependences of the polar-cap luminosity $\log(L_{\text{tot}}/\text{erg/s})$ (left) and the efficiency $\log(L_{\text{tot}}/\dot{E})$ (right), where $\dot{E}$ is the loss rate of the star's rotational energy, on the height where the region of total screening begins $z_r = \eta_r - 1$ for the case $B_0 = 2 \times 10^{12}$ G, $P = 1$ s, $\chi = 10°$. The case $z_r = z_c$ corresponds to computing L_{tot} in the strong-screening model. Lower: corresponding values of the reverse positron current $\log A_{\text{rev}}$ (left) and the characteristic surface temperature T, K (right).

imation: $Err_0(u) = (F_0(u) - F_0^{app}(u))/F_0(u)$ and $Err_1(u) = (F_0(u) - F_1^{app}(u))/F_1(u)$, respectively.

Figure 4 shows examples of the dependences of L_{tot}, A_{rev}, and the characteristic surface temperature T_{eff} on the height η_r for the case $B_0 = 2 \times 10^{12}$ G, $P = 1$ s, $\chi = 10°$. The height of the upper plate z_c was computed analogous to how this was done in [36]. When finding the height of the upper plate, only the creation of electron–positron pairs via of absorption of curvature radiation from primary electrons in the presence of the magnetic field (the CR case) was taken into account. The function $f(\eta)$ was computed using (18), and the temperature T was estimated from the relation $L_{\text{tot}} = \sigma_B T^4 \pi \theta_s^2 a^2$.

7. CONCLUSION

We have considered the method for computing the reverse current [8] with the model of the inner gap proposed in [21]. The resulting expressions for the reverse current when using the SS model more or less coincide with those from [8, 9]. However, expression (53) differs from formula (33) in [9] by a factor of two. This is probably due to the different methods used here and in [9] to take into account

the contribution of the term $\theta_s^2(\eta_c) \left.\frac{\partial^2 \Phi}{\partial \eta^2}\right|_{\eta=\eta_c}$. Expression (52) is in reasonable agreement with the estimate $A_{\text{rev}} \sim \kappa \theta_s$ presented in [12], but differs appreciably from the expression $A_{\text{rev}} = \frac{\kappa}{2}\left(1 - \frac{1}{\eta_c^3}\right) A_{\text{prim}}$ obtained using Eqs. (3) from [29]. Even when $\xi = 0$, expression (52) predicts a reverse current that is a factor of $\sim 1/\theta_s \sim 10^2$ lower than the value obtained in [29]. This difference is due to the fact that the contribution of the perpendicular part of the Laplacian $\Delta_\perp \Phi$ was not included when finding the reverse positron current in [29]. Both expressions were obtained under the assumption $z_c \gg \theta_s$. However, the condition $\Delta_\perp \Phi \approx -4\pi(\rho - \rho_{GJ})$ [21]—i.e., essentially the screening condition (40)—is then satisfied with very good accuracy slightly below the upper plate. Accordingly, in full agreement with [8], the reverse positron current only needs to cancel out the small term $\theta_s^2(\eta_c) \left.\frac{\partial^2 \Phi}{\partial \eta^2}\right|_{\eta=\eta_c}$, and not the full quantity $\Delta\Phi$, as was assumed in [29].

The results of the computation of the current in the WS model are in reasonable agreement with the computations of [10]. In this case, the reverse current is determined mainly by the large difference $f(\eta_r^{WS}) -$

$f(\eta_c)$; whether or not the terms $\theta_s^2(\eta_c)\left.\frac{\partial^2 \Phi}{\partial \eta^2}\right|_{\eta=\eta_c}$ and, when $z_c \ll 1$, as is assumed [10], $\Delta_\perp \Phi$ are taken into account influences the final result only weakly.

We have considered heating of the caps only for the CR case, so that the pulsar is taken to lie to the left of the curvature-radiation line of death. For a dipolar magnetic field ($\nu = 0$), this line has the form [44]

$$P = 0.16\left(\frac{B_0}{10^{12}\,\text{G}}\right)^{4/7}\cos^{3/7}\chi \quad \text{s.} \qquad (69)$$

In the presence of a small-scale field, its position can be estimated as [44]

$$P \approx (0.5{-}1.0)\left(\frac{B_0}{10^{12}\,\text{G}}\right)^{2/3} \quad \text{s.} \qquad (70)$$

Note that, in the CR case, the screening of $E_\parallel$ is due mainly to particles with relatively small energies $E_\pm^{CR} \sim (10^2{-}10^4)mc^2$, whose number rises very rapidly near the upper plate of the diode z_c (with a characteristic scale $\sim 1{-}10$ m $\ll z_c a$) [9, 10]. As a result, the potential Φ in the region $z > z_c$ increases only by an amount $\delta\Phi \sim \frac{E_\pm^{CR}}{e} \sim (10^2{-}10^4)\frac{mc^2}{e} \ll \Phi|_{z=z_c}$ [9, 10]. In this situation, pairs created by inverse Compton radiation essentially do not participate in the screening of $E_\parallel$. The reason is that these pairs have energies $E_\pm^{IC} \sim (10^2{-}10^4)E_\pm^{CR}$ ($E_\pm^{IC} \sim e\,\Phi|_{z=z_c}$) [33], and the weak electric field in the region $z > z_c$, $e\delta\Phi \sim (10^{-2}{-}10^{-4})E_\pm^{IC} \ll E_\pm^{IC}$, is not able to effectively slow down, much less reverse, test particles. Electron−positron pairs created by synchrotron radiation likewise essentially do not participate in screening of $E_\parallel$. This is so because the particles move with nearly zero pitch angles in the region of the inner gap and, when $B_0 < 4 \times 10^{12}$ G, the synchrotron photons in this region are mainly emitted by electron−positron pairs that are excited to Landau levels. Consequently, these photons arise in appreciable numbers only when $z \gtrsim z_c$, and only with modest energies (comparable to the energies of curvature-radiation photons). Therefore, pairs created from curvature photons will appear in appreciable numbers only at large heights $z - z_c \gtrsim \frac{1}{3}z_c$, where $E_\parallel$ is already nearly completely screened.

We also assumed that we can neglect the birth of particles in the region of the diode $0 < z < z_c$. If such particles are created by the NICR mechanism, a sufficient condition for this to be valid is that the surface temperature of the star not be too high,

$$T \lesssim 3 \times 10^6 \left(\frac{\Gamma_c}{10^6}\right)^{1/2}\left(\frac{10^{-2}}{z_{\min}^{NIC}}\right)^{1/2}\,\text{K}, \qquad (71)$$

where $z_{\min}^{NIC} = \min(z_c, \theta_0)$ in the case of scattering on photons from a polar cap and $z_{\min}^{NIC} = \min(z_c, 1)$ and $\Gamma_c = \left.\frac{e\Phi}{mc^2}\right|_{z=z_c,\xi=0}$ in the case of photons coming from the surface of the entire star. Moreover, it was assumed that the energy density of radio emission trapped in the diode U_{rad} [45] is not sufficiently high to appreciably influence the acceleration of particles in the region $0 < z < z_c$ [45],

$$U_{\text{rad}} \ll 10^8 \left(\frac{10^{-2}}{z_c}\right)\left(\frac{10^6}{\Gamma_c}\right)\frac{\text{erg}}{\text{cm}^3}. \qquad (72)$$

Note also that we neglected the effect of thermal radiation pressure on the particles [46] and the possibility of pair creation in bound states. This last effect could be very important when $B > (4{-}6) \times 10^{12}$ G [47].

Our study did not take into account the influence of outer gaps on heating of the polar caps. In real pulsars, it is likely that part of the tube is occupied by outer gaps (which may already be switched off in old pulsars; see, e.g., [1, 48, 49]). On the one hand, the presence of outer gaps means that the inner gap occupies only part of the pulsar tube [1, 39]. For example, the case when the inner gap occupied only $\sim(50{-}70)\%$ of the transverse cross section of the pulsar tube, depending on the inclination χ, was considered in [50]. Accordingly, the contribution of the inner gap to heating the polar caps could be roughly a factor of $1.5{-}2$ lower. On the other hand, some of the reverse positron current could pass through the outer gaps. Since, generally speaking, the outer gaps can accelerate electrons moving from behind the light cylinder to energies ~ 100 GeV-1 TeV, even in the switched-off state, this could lead to additional heating of the polar caps [1, 39]. Moreover, we have not considered heating of the polar caps by the current of relativistic positrons or protons A_{proton} coming from behind the light cylinder along the magnetic-field lines on which the inner gap is located [51]. Note that the presence of such a current simply leads to renormalization of the primary electron current, $A_{\text{prim}} \to (A_{\text{prim}} - A_{\text{proton}})$; accordingly, the associated additional heating can be computed using (64) with the substitution $f(\eta_r^{WS}) - f(\eta_c) \to \frac{1}{2}A_{\text{proton}}$.

The weakest aspect of our current study is the assumption that all quantities are independent of time (in a coordinate frame rotating together with the neutron star). Although there are quantitative arguments supporting the stability of the inner gap ([52]; E.M. Kantor, private communication), numerical simulations [53, 54] appear to support the idea that the gap operates in a non-stationary regime [3]. According to [53], the non-stationarity in the gap is due to the fact that, even in the case of free outflow, sparks are continuously ignited and extinguished in

the gap. A similar regime was considered in [27, 28]. According to [53], in the non-stationary regime, the reverse positron current exceeds the value we have obtained in this study. This is quite natural (V.S. Beskin, private communiction), since the appearance of oscillations is related to a large extent to the fact that the reverse positron current stops the outflow of electrons from the neutron-star surface. Consequently, the value $A_{\rm rev}$ should exceed the Goldreich−Julian density, $f(1) \sim 0.5-1.0$ [3], which appreciably exceeds even the reverse current computed in the WS model. However, since the particles arrive at the polar cap mainly in the extinguishing phase of the sparks [53], when the plasma nearly completely screens the electric field, the total heating of the caps is modest in the non-stationary case, comparable to the heating in the SS model to order of magnitude.

In spite of this support from numerical simulations, we believe that non-stationary models encounter one large problem. Very strong oscillations in the electric field can occur in such models, and the particle number density also varies very strongly. According to [53], sparks should continuously be extinguished and ignited anew. In our view, it is very difficult for an ordered structure to survive over prolonged times in such a medium with continuously varying parameters (on time scales $\sim c/z_c \sim 10^{-6}-10^{-4}$ s). However, we know from observations of sub-impulse drift that ordered structures exist in at least some pulsars [55, 56]; in order to observed a drift in P_4, these structures must not undergo substantial variations, at least over times $\sim P_4 \sim 10-40$ s [6, 20]. Therefore, in our view, the very fact that sub-impulse drift of the period P_4 is sometimes observed may testify to the fact that the electric fields and particle number densities in pulsar tubes do not undego very large variations on time scales $\sim c/z_c$, making stationary models a relatively good approximation.

ACKNOWLEDGMENTS

REFERENCES

1. S. Shibata, Astrophys. J. **378**, 239 (1991).
2. V. S. Beskin, *Axisymmetric Stationary Flows in Astrophysics* (Fizmatlit, Moscow, 2006) [in Russian].
3. P. A. Sturrock, Astrophys. J. **164**, 529 (1971).
4. J. A. Gil and M. Sendyk, Astrophys. J. **541**, 351 (2000).
5. J. Gil, G. Melikidze, and B. Zhang, Mon. Not. R. Astron. Soc. **376**, L67 (2007).
6. J. Gil, F. Haberl, G. Melikidze, U. Geppert, B. Zhang, and G. Melikidze, Jr., Astrophys. J. **686**, 497 (2008).
7. W. M. Fawley, J. Arons, and E. T. Scharlemann, Astrophys. J. **217**, 227 (1977).
8. J. Arons and E. T. Scharlemann, Astrophys. J. **231**, 854 (1979).
9. A. K. Harding and A. G. Muslimov, Astrophys. J. **556**, 987 (2001).
10. D. P. Barsukov and A. I. Tsygan, Astron. Rep. **47**, 1046 (2003).
11. P. Goldreich and W. H. Julian, Astrophys. J. **157**, 869 (1969).
12. J. A. Hibschman and J. Arons, Astrophys. J. **554**, 624 (2001).
13. B. Zhang, A. K. Harding, and A. G. Muslimov, Astrophys. J. **531**, L135 (2001).
14. V. Urpin and J. Gil, Astron. Astrophys. **415**, 305 (2004).
15. A. Bonanno, V. Urpin, and G. Belvedere, Astron. Astrophys. **440**, 199 (2005).
16. U. Geppert, M. Rheinhardt, and J. Gil, Astron. Astrophys. **412**, L33 (2003).
17. M. Rheinhardt and U. Geppert, Astron. Astrophys. **435**, 201 (2005).
18. E. Asseo and D. Khechinashvili, Mon. Not. R. Astron. Soc. **334**, 743 (2002).
19. J. Gil, G. Melikidze, and B. Zhang, Astron. Astrophys. **457**, L5 (2006).
20. A. Szary, arXiv:1304.4203 [astro-ph.HE] (2013).
21. E. M. Kantor and A. I. Tsygan, Astron. Rep. **47**, 613 (2003).
22. M. A. Ruderman and P. G. Sutherland, Astrophys. J. **196**, 51 (1975).
23. Z. Medin and D. Lai, Adv. Space Res. **40**, 1466 (2007).
24. J. A. Gil, G. I. Melikidze, and U. Geppert, Astron. Astrophys. **407**, 315 (2003).
25. R. X. Xu, B. Zhang, and G. J. Qiao, Astropart. Phys. **15**, 101 (2001).
26. J. W. Yu and R. X. Xu, Mon. Not. R. Astron. Soc. **414**, 489 (2011).
27. Ya. N. Istomin and D. Sob'yanin, J. Exp. Theor. Phys. **113**, 592 (2011).
28. Ya. N. Istomin and D. Sob'yanin, J. Exp. Theor. Phys. **113**, 605 (2011).
29. V. D. Pal'shin and A. I. Tsygan, Preprint FTI im. A.F. Ioffe No. 1718 (Fiz. Tekh. Inst., St.-Petersburg, 1998).
30. J. A. Gil, G. I. Melikidze, and D. Mitra, Astron. Astrophys. **388**, 235 (2002).
31. G. Melikidze, J. Gil, and A. Szary, Rev. Mex. Astron. Astrofis., Ser. Conf. **36**, CD337 (2009).
32. A. K. Harding and A. G. Muslimov, Astrophys. J. **508**, 328 (1998).
33. A. K. Harding and A. G. Muslimov, Astrophys. J. **568**, 862 (2002).

34. E. T. Scharlemann, J. Arons, and W. M. Fawley, Astrophys. J. **222**, 297 (1978).

35. A. G. Muslimov and A. I. Tsygan, Mon. Not. R. Astron. Soc. **255**, 61 (1992).

36. D. P. Barsukov, E. M. Kantor, and A. I. Tsygan, Astron. Rep. **51**, 469 (2007).

37. Yu. E. Lyubarskii, Astron. Astrophys. **261**, 544 (1992).

38. Yu. Lyubarskii, Astrophys. Space Sci. **342**, 79 (2012).

39. S. Yuki and S. Shibata, Publ. Astron. Soc. Jpn. **64**, No. 43 (2012).

40. G. Z. Machabeli, Q. Luo, S. V. Vladimirov, and D. B. Melrose, Phys. Rev. E **65**, 036408 (2002).

41. G. Z. Machabeli and G. T. Gogoberidze, Astron. Rep. **49**, 463 (2005).

42. I. F. Malov, *Radiopulsars* (Nauka, Moscow, 2004) [in Russian].

43. I. F. Malov and E. B. Nikitina, Astron. Rep. **56**, 693 (2012).

44. E. M. Kantor and A. I. Tsygan, Astron. Rep. **48**, 1029 (2004).

45. V. M. Kontorovich and A. B. Flanchik, JETP Lett. **85**, 267 (2007).

46. M. A. Garasyov, E. V. Derishev, and V. V. Kocharovskii, Astron. Lett. **34**, 305 (2008).

47. V. V. Usov and D. B. Melrose, Austral. J. Phys. **48**, 571 (1995).

48. K. Hirotani, Mod. Phys. Lett. A **21**, 1319 (2006).

49. R. B. Wang and K. Hirotani, Astrophys. J. **736**, id 127 (2011).

50. G. J. Qiao, K. J. Lee, H. G. Wang, R. X. Xu, and J. L. Han, Astrophys. J. **606**, L49 (2004).

51. K. Asano and F. Takahara, Astron. Astrophys. **428**, 139 (2004).

52. K. Hirotani, Astrophys. J. **549**, 495 (2001).

53. A. N. Timokhin and J. Arons, Mon. Not. R. Astron. Soc. **429**, 20 (2012).

54. A. Levinson, D. Melrose, A. Judge, and Q. Luo, Astrophys. J. **631**, 456 (2005).

55. J. M. Rankin and R. Ramachandran, Astrophys. J. **590**, 411 (2003).

56. D. Mitra and J. M. Rankin, Mon. Not. R. Astron. Soc. **385**, 606 (2008).

Translated by D. Gabuzda